

# Plasmonic Enhancement of Vibrational Excitations in the Infrared

Frank Neubrech and Annemarie Pucci

(Invited Paper)

**Abstract**—Related to their size and shape, plasmonic excitations of metal particles occur in an extremely broad spectral range from visible down to radio frequencies. They can couple to other kinds of excitation with a similar energy, which in the infrared (IR) is origin of vibrational signal enhancement. In this study, we recollect main points of the current knowledge on such coupling and give examples with molecular vibrations and phonons. Plasmonic enhancement of various phononic signals gives rise to distinguish between surface enhanced IR absorption and surface enhanced IR scattering.

**Index Terms**—Antennas, electromagnetic coupling, infrared (IR) spectroscopy, optical sensors.

## I. INTRODUCTION

INFRARED (IR) spectroscopy is used for more than 100 years, mainly for vibrational spectroscopy. IR photons can excite vibrations of the same energy from a lower (usually the ground state) to a higher level. So IR spectra reveal absorption lines from all those specific vibrations that can couple to the incoming photons. In solids, vibrational excitations exist as phonon waves. In an excitation process, energy, wave vector, and polarization have to be conserved. These points are already known for many decades. For solids with optical phonons, IR optical properties mainly depend on phonon properties—consider, for example, the reststrahl region between the longitudinal LO and the transverse TO optical phonon frequencies with its high reflectivity. Therefore, for optical phonon-data bases, reflectance studies were used. Another data source is thin-film studies that yield TO frequencies  $\omega_{\text{TO}}$  and, at oblique incidence, via the Berreman effect [1], also LO frequencies  $\omega_{\text{LO}}$  from thin-film polariton excitation. In current studies of bulk vibrations with IR spectroscopy, in combination with calculations of the electronic structure of the ground state, motivation is it to learn about the atom-geometric structure and bonding in the condensed system, like, for example, new organic semiconductors [2], [3]. In surface science and catalysis, adsorbate bonding

to a substrate or host is an important issue and any shift and line-shape change of vibrational signals may inform on charge transfer and chemical bonding to the surface (or host) [4]. We also have to mention here that current IR spectroscopy includes low-energetic electronic excitations [5]–[7] and IR plasmonic studies, see below. A manifold of spectroscopic techniques is available nowadays: time-resolved techniques [8], microscopy in the far- and the near-field [9], and nonlinear methods like sum-frequency generation [10].

In studies related to sensing of small amounts of molecules, for example in order to identify rare biomarkers, IR spectroscopy suffers from relative low vibrational absorption signals compared to noise (S/N). Absorption cross sections typically are well below  $1 \text{ nm}^2$ , which is about 11 orders of magnitude smaller than a possible IR beam focus. Nowadays, modern IR techniques provide the photometric sensitivity to detect intensity changes down to  $10^{-4}$ . Missing orders of magnitude can be bridged by IR lasers only partially. One efficient way to increase sensitivity is to exploit near-field enhancement from resonant particles in the neighborhood of molecules of interest. Two kinds of excitations support resonant behavior of particles in the IR: phonon-like and plasmon-like surface polaritons [11]–[13]. Polariton excitation benefits from a low imaginary part of the dielectric function (low damping) and from a negative real part of that function. Concerning phonon excitation at room temperature, such conditions are well met in the case of crystalline SiC. For plasmonic excitations in the IR, almost all good metal conductors can be used. Plasmonic near-fields are strongly enhanced at resonance by up to two to three orders of magnitude [14]–[17], which for IR absorption spectra would mean up to six orders of vibrational signal enhancement can be expected. But experimental facts are not fully consistent with such simple picture because of the strong line-shape changes of enhanced vibrational signals [18], [19], see also for example Fig. 1. These line-shape changes show Fano-type profiles and, with nanoantennas, they can reach antiabsorption [20]. Furthermore, particle-plasmon polaritons can couple to phonon polaritons with wave-vector direction perpendicular to the incoming photon wave vector. In the following, we will explain these effects more detailed and discuss consequences for sensing.

## II. PLASMONIC INTERACTION IN THE IR

### A. IR Plasmonic Resonances

Below the onset of interband transitions the IR optical conductivity of metals is determined by collective oscillations of free charge carriers called plasmons. These plasmonic

Manuscript received July 31, 2012; revised September 26, 2012; accepted October 23, 2012. Date of publication November 16, 2012; date of current version April 25, 2013. This work was supported in part by the European Union project NANOANTENNA under Program HEALTH-F5-2009-241818 and by the German Science Foundation under DFG PU193/9-1 and DFG PU193/12-1.

F. Neubrech is with the Kirchhoff Institute for Physics, Heidelberg University, 69120 Heidelberg, Germany, and also with Stuttgart University, 70174 Stuttgart, Germany (e-mail: neubrech@kip.uni-heidelberg.de).

A. Pucci is with the Kirchhoff Institute for Physics and Centre for Advanced Materials, Heidelberg University, 69120 Heidelberg, Germany (e-mail: pucci@kip.uni-heidelberg.de).

Color versions of one or more of the figures in this paper are available online at <http://ieeexplore.ieee.org>.

Digital Object Identifier 10.1109/JSTQE.2012.2227302

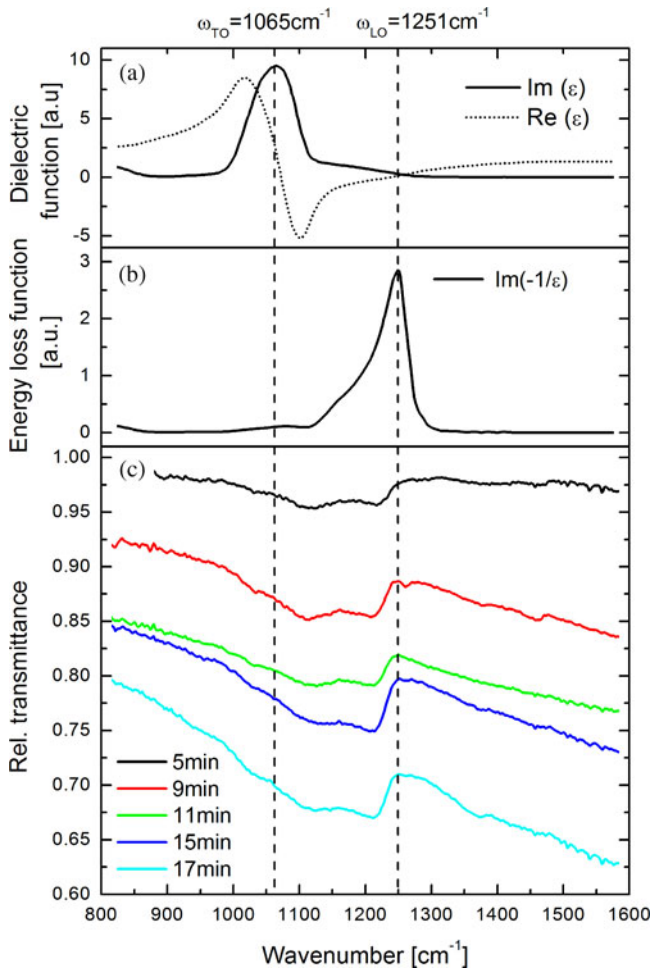


Fig. 1. (a)  $\text{SiO}_2$  complex dielectric function and (b) energy loss function. Maxima positions are marked. The range between them is the reststrahl region of the Si–O stretching mode of amorphous  $\text{SiO}_2$ . Relative IR transmittance of wet-chemically grown Au-island films on a silicon wafer with about 3-nm-thick natural oxide. (c) Growth time is indicated. Incidence of light is normal, reference is the wafer without gold. While phonon absorption in 3-nm silicon oxide gives only a signal of 0.01 compared to pure silicon surfaces, the much stronger feature between 1000 and 1250  $\text{cm}^{-1}$  is due to plasmonic enhancement. Its special line shape tells that the mechanism is more complicated than simple enhancement. It is important to note that an ultrathin flat gold layer would lead to oxide vibrational feature toward higher relative transmittance due to screening of the incoming field.

oscillations give rise to the high metallic reflection up the plasma edge [22]. Electromagnetic waves with frequencies below the plasma edge are attenuated inside the metal. However, within the penetration depth of a few 10-nm, surface-plasmon polaritons as mixed excitations of plasmonic and photonic nature can also exist in the IR range [23], [24]. The Drude dielectric function allows a good description of the optical plasmonic response with only two parameters (plasma frequency and relaxation rate of free charge carriers) if the extension of the nanostructure is larger than a few nanometers [25]–[27]. For almost all metals, the dielectric function has a very strong negative real part in the IR. In the mid IR, for the most metals, the absolute value of this real part is much larger than the imaginary part that gives electronic damping of plasmonic excitations and limits the polariton propagation length. Nevertheless, for good metals in the

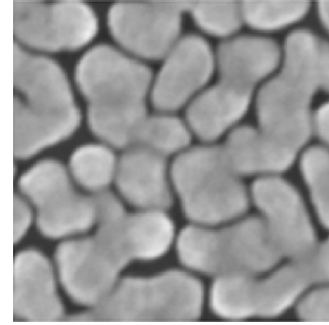


Fig. 2. Scanning electron microscopy (SEM) image of a typical SEIRA-active wet-chemically grown Au-island layer on an Si wafer, ca. 350 nm  $\times$  350 nm. A monolayer of APTES was used to improve gold nanoparticle adhesion [21].

mid IR, the propagation length on a smooth surface is much larger than the wavelength, but surface roughness may shorten it [28]. Electronic damping can be decreased by a lowered defect concentration in the bulk and on the surface and it is always lower for suppressed phonon scattering at low temperatures [29].

On extended surfaces, propagating plasmon–polaritons can be optically excited by well-established techniques (e.g., Otto configuration) that ensure energy and momentum conservation [30], [31]. Refractive-index sensing applications of these techniques are well established [32], [33]. They exploit the strong influence of the electronic polarizability of the neighbor medium on the plasmon–polariton dispersion relation.

Plasmon–polaritons become localized on metal particles and for the plasmon–polariton wave vectors only such of standing waves are allowed. Thus, plasmonic excitations correspond to collective charge oscillation modes of various orders of standing waves. These resonances depend on size and shape of the particle [34], [35] but also on the material quality [36]. The two limiting cases are, one the one side, macroscopic radio-frequency antennas where only geometry is important [37], and on the other side, nanoparticles at least 100 times smaller than the photon wavelength with Mie resonances in the Rayleigh limit depending almost only on the materials properties [38], [39].

For complex metal particle structures, coupling of different modes can be achieved via Fano-type interaction effects (see below). The Fano-type coupling between dark and bright plasmon-modes transfers optical activity to the dark mode, which may give rise for very narrow plasmonic resonances as they are advantageous for refractive index sensing [40], [41]. Mutual plasmonic coupling can be nicely studied with precisely top-down manufactured nanostructures [42].

In the past, many studies were dealing with bottom-up grown nanoisland films, see for example Fig. 2. These films are more or less disordered 2–D arrays of interacting plasmonic particles and, with further metal deposition, changes in island size, shape, and mutual interaction modify the optical response dramatically [43], [44]. In the IR, this optical behavior can be exploited for contact-free measurement of electrical percolation. Very close to the percolation threshold [45] distances between metal islands are extremely small [46], which is beneficial for near-field enhancement. The normal-incidence IR transmittance at percolation is nearly frequency independent, which can be

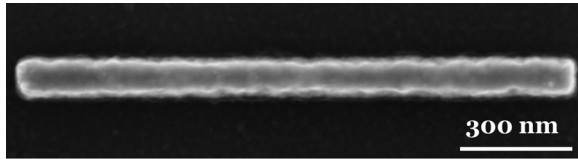


Fig. 3. SEM of a typical electron-lithographically produced gold antenna (on silicon wafer with natural oxide, 10-nm Ti adhesion layer between gold and silicon oxide) [50].

attributed to the overlap of two contributions, one from separate islands and the second one from the fully coalesced area [47]. Local field enhancement spatially varies on the layer in relation to morphology [48]. Modification of morphology, for instance at percolation, is possible via flux and diffusion of metal atoms [49]. So, metal-island films can be properly produced to be a cheaper alternative to nanolithographic structures for surface enhanced vibrational spectroscopy. Spectra usually are measured in transmittance geometry and, for adsorbate-covered metal-island films (on a transparent substrate), the signals almost resemble an absorption increase, which lead to the term “surface enhanced IR absorption (SEIRA).”

A very interesting approach to SEIRA-active substrates is based on dense hexagonal arrays of identical particles, for example, core-shell spheres the resonance of which is governed the shell thickness and particle diameter [51], [52].

It is still under debate which metal-particle geometry and arrangement produces the highest near-field. Small longitudinal gaps of a few nanometer width are proven to be advantageous [53]. But quantum theory predicts a minimum distance below which the near-field decreases again [54], [55].

Modern techniques enable the production of well-defined nanostructures in homogeneous arrays. Hence, measurements and simulations can be precisely compared, which gave a lot of important insights into plasmonic resonances and their tuning, plasmonic couplings, and near-field concentration [42], [56], [57].

The simplest elements for tunable IR near-field enhancement are nanowires (example in Fig. 3) with length  $L$  in the micron-range [58]–[60]. They show strong fundamental resonances with an almost linear antenna-like relation  $\lambda_{\text{res}} = AL + B$  (with  $B$  less important in the IR) between photon wavelength  $\lambda_{\text{res}}$  at resonance and  $L$ , see Figs. 4 and 5. The parameters depend on plasma frequency, substrate polarizability, cover layers, and geometry details like width  $w$  and height  $h$ . A corresponding analytic formula was derived by L. Novotny for cylindrical wires and penetration depths clearly smaller than the wire diameter [37].

From Figs. 4 and 6, it is obvious that extinction cross sections of a nanowire at resonance exceed geometric ones considerably, which is proving the strong near-field concentration at resonance. From many theoretical studies and from scanning near-field optical microscopy, it is known that near-field enhancement at resonance is localized next to the nanowire apex and it is maximum for the fundamental resonance [20], [61], [62]. For enhanced vibrational spectroscopy thus the fundamental antenna-type resonances are best suited [20], [63]. Nanowires and also other kinds of particles, like nanocrescents [64], show

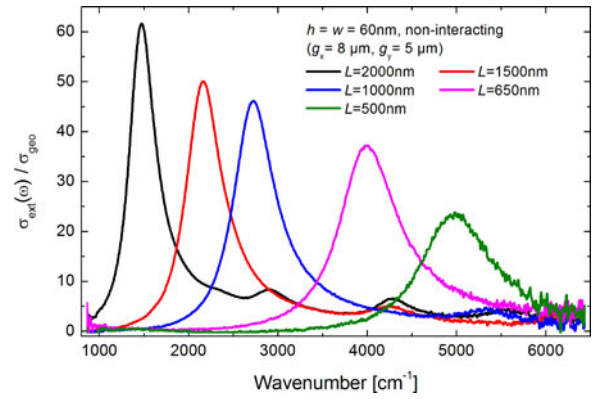


Fig. 4. Experimental extinction cross section related to the geometrical one of gold nanoantennas with different lengths  $L$ , height  $h$ , and width  $w$  (given in the figure) on a  $\text{CaF}_2$  substrate. The measurements of the nanoantennas were done under normal incidence of light with an electrical field vector parallel to the long antenna axis. The longitudinal and the horizontal distances are  $g_x = 8$  and  $g_y = 5 \mu\text{m}$ , respectively, which is too large for remarkable mutual interaction. Strongest maxima in extinction indicate fundamental plasmonic resonances.

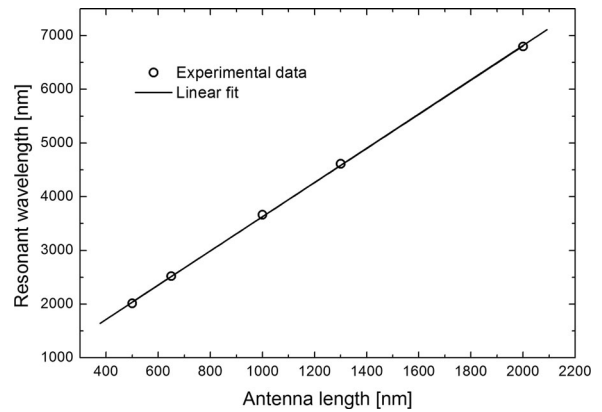


Fig. 5. Resonance photon wavelength  $\lambda_{\text{res}}$  as extracted from the spectra shown in Fig. 4. The linear relation  $\lambda_{\text{res}} = 3.178[1/\text{nm}] \times L + 451 \text{ nm}$  gives a perfect fit to the data.

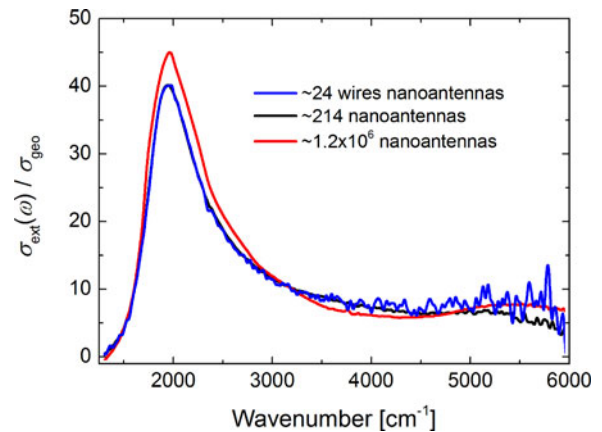


Fig. 6. Extinction cross section normalized to the geometrical one for different numbers of illuminated nanoantennas ( $L = 800 \text{ nm}$ , width and height  $100 \text{ nm}$ , transverse distance  $5 \mu\text{m}$ , longitudinal distance  $1 \mu\text{m}$ ) on a Si wafer. For the largest number of nanoantennas, no Schwarzschild optics was used. The diameter of the Gaussian IR beam was similar to the  $4 \text{ mm} \times 4 \text{ mm}$  array dimension. For the lower numbers of antennas,  $\text{NA} = 0.5$  and different apertures were used in the IR microscope.

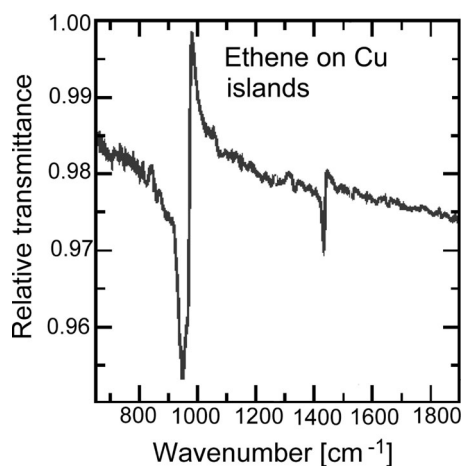


Fig. 7. SEIRA of condensed ethene (5.4 Langmuir exposure at 50 K) on Cu-island film on KBr. The Cu layer is close to percolation. It was deposited at room temperature and corresponds to 8.6-nm average thickness. Reference is the bare-island layer [65].

remarkable enhancement. The main differences to SEIRA-active layers from densely packed nanoparticles (with overall extension much smaller than the wavelength) are pronounced resonant scattering and spectral selectivity. Because of the latter, nanoantennas enhance only vibration signals with a good frequency match to the plasmonic resonance spectrum.

Experimental spectra shown in this study are measured in normal transmittance geometry. For IR microscopy light was focused with a Schwarzschild objective with numerical aperture  $NA = 0.5$ . This kind of mirror optics in reality leads to slight deviations from normal incidence. Therefore, arrays with transversal and longitudinal distances between nanowires tuned to interference maxima for normal incidence show considerable differences in spectra for different NA [66]. Fig. 6 shows experimental extinction for a very homogeneous extended array that is not diffractively coupled. Microspectroscopic measurements are compared to spectra taken without Schwarzschild optics but with an almost parallel beam. Up to 10% deviation in extinction cross section is observed. For detailed nanoantenna studies and comparison to theory, such kind of deviation and the real beam profile should be considered.

### B. Fano-Type Interaction

The open problem that still hampers broad application of surface enhanced IR spectroscopy is the missing precise quantitative information on the number of oscillators that contribute to the signal. In fact, the enhancing mechanism is more than simply near-field enhancement. Therefore, the enhancement factor cannot be directly estimated from the plasmonic near-field. In particular, from SEIRA with island films (see, e.g., Fig. 7), a clearly Fano-type vibrational line shape is obvious [18], [19], [65]. The deviation from a Lorentzian line shape toward a Fano-type one increases with vibrational signal enhancement, in accordance to the Fano-interference effect that yields intensity transfer from a continuum to a narrow oscillator and a significant line-shape change of the narrow oscillator up to full asymmetry or even

antiabsorption. Empirically, the asymmetry is described by the Fano parameter that corresponds to the ratio of the transition probabilities for the two excitations. Without continuum (i.e., without plasmonic excitation), this parameter becomes infinity and the narrow line shape is the typical Lorentzian. Fano effects are found for various kinds of excitations in nature and enable fascinating new properties, for example [40], [67]–[69]. Even dark modes may become bright from intensity transfer, as mentioned earlier.

In SEIRA, maximum asymmetry and maximum vibrational signals were found for island layers near percolation [19], see Fig. 7. The Fano-type shape and the vibrational intensity could be well simulated by a simple 2-D Bruggeman model [19] that neglects details of the metal-particle shape and scattering, which is a reasonable approximation for islands with dimensions two orders of magnitude smaller than the IR wavelength. It is important to note that this simple Bruggeman simulation succeeds in an accordance to experimental findings only if the bare-film spectrum can be simulated in good agreement too [19], [70]. This rule works better for small islands or for metals with electronic scattering rates in the mid IR (like e.g., iron), respectively. With increasing gas exposure a linear increase in the SEIRA signal of ethene on Cu islands on KBr (see Fig. 7) up to at least 20 Langmuir was observed [71]. IR active modes in the mid IR are equally enhanced and show the same asymmetry [19]. Quantitative analysis on metal-island films is limited by an irregular distribution (and possibly orientation) of analyte molecules over the various sites with different near-field enhancement. Furthermore, one has to consider that the number of adsorption sites depends on morphology. So, the obvious signals in SEIRA studies for different morphologies usually include various amounts of adsorbate molecules.

Concerning plasmonic enhancement with nanoantenna-like resonantly scattering objects, vibrational-signal increase is much larger, but quantitative analysis is much less clear [20], [63], [64], [68], [72]. Recent experiments indicate that the scattered far-field intensity goes with the fourth power of the near-field strength [73]. For a vibrational signal from a molecule in the enhanced near-field this finding would mean that two effects contribute to vibrational signal enhancement, one ordinary from enhanced absorption (SEIRA) that goes with the square of near-field enhancement and a second one that is the modified scattering which goes with the fourth power of near-field enhancement. This second effect we will call surface enhanced IR scattering (SEIRS). Clearly, in total, for resonant antennas the second effect, SEIRS, should dominate. As will be discussed later, the two contributions can be separated because they differently involve wave vectors.

From experiments, it is known that SEIRS with nanoantennas is also a Fano-type effect [20]. Fano-type line shapes are observed, see Figs. 8 and 9. With detuning of vibrational and plasmonic resonance line shape and signal size change as qualitatively predicted for a Fano effect. For the best tuning condition in Fig. 8, even a signal from the octadecane thiol (ODT)  $\text{CH}_3$  group at  $2963 \text{ cm}^{-1}$  is observed. Please note, there is only one such group per molecule. Differently to Fano-type SEIRA signals from adsorbates on metal-island layers, for nanoantennas

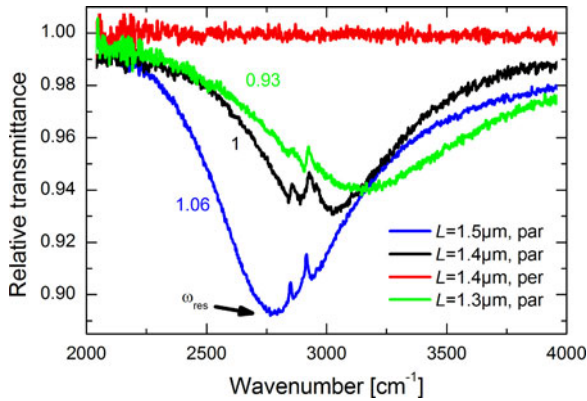


Fig. 8. Polarization-dependent relative transmittance spectra of individual electro-chemically grown gold nanoantennas (with various length  $L$  as given) covered with a monolayer ODT [20]. Besides the broadband plasmonic response, narrow spectral features are found at  $2855$  and  $2929$   $\text{cm}^{-1}$  which can be assigned to  $\text{CH}_2$  stretching vibrations of ODT. Depending on the tuning ratio (given as the frequency ratio of plasmonic resonance and the vibrational excitation, approximate numbers are given), differently looking vibrational signals appear on the plasmonic background.

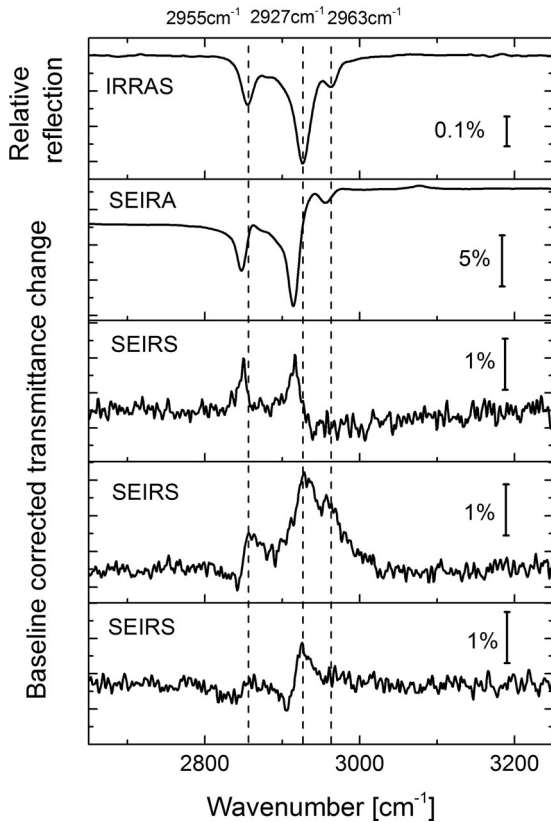


Fig. 9. Baseline-corrected vibrational signals of the  $\text{CH}_2$  and  $\text{CH}_3$  vibrational modes of one monolayer of ODT for different measurement geometries as indicated in each panel. The IR reflection absorption spectroscopy (IRRAS), where a large area with ODT molecules contribute to the signal acts as reference signal for SEIRS [74]. In the case of SEIRA [21], adsorbates on sidewalls of island on a  $\text{cm}^2$ -sized sample area contribute to the signal [18], [21]. For SEIRS on gold nanowires, the signal strength as well as the line-shape strongly depends on tuning. The vibrational signal arises from the apex of the nanowires where the near-field is strongly enhanced. SEIRS spectra from Fig. 8 after baseline correction, same sequence from top to bottom.

maximum signals have an antiabsorption line shape, i.e., the vibrational oscillator has to be considered as in an antiphase condition in order to explain weakening of plasmonic extinction.

Looking at the parameters that govern the Fano effect may be helpful for optimizing SEIRS enhancement. Many studies in the recent years and some comprehensive reviews were dealing with the influence of damping and of coupling on the spectrum [67]–[69], for example, in relation to exciton-plasmon coupling [76], [77]. For the “plexitonics” case [76], [77], it was clearly demonstrated that the Fano-type signal disappears with broadening of the narrow oscillator. Transferred to a system with molecular adsorbate layers this finding means stronger SEIRA and SEIRS are possible for well-ordered layers with intrinsically narrow vibrational lines. In contrast, water adsorbed under ambient conditions never was detected in SEIRS experiments, certainly because of the very broad vibrational bands. Also, the application of SEIRS to vibrational sensing of biomolecules is hampered related to their broad vibrational features, for example [78].

Extremely important is the coupling between the two interfering excitations in the Fano effect. Strong coupling can even lead to Rabi splitting, as explained for the coupling between excitonic emission and plasmonic excitation [76], [77], for example. Following the references, the criterion for strong coupling is approximately described as  $g > \gamma_{pp}/4$  with  $g$  as the coupling rate between the two excitations (the narrow excitonic one and the broad plasmonic one) and  $\gamma_{pp}$  as the decay rate of the plasmonic resonance (if described as harmonic oscillator). If there are  $N$  excitonic oscillators that interact with the plasmonic excitation, the coupling strength becomes  $g\sqrt{N}$ . The squared coupling strength  $g^2$  is proportional to the spontaneous excitonic emission rate and to the enhancement of the field-mode density at the spatial position and the vacuum resonance frequency of the excitonic emitter [77]. Translated into terms of vibrational excitations,  $g^2$  is proportional to the near-field enhancement and to the vibrational oscillator strength. This approximate picture is not complete. In reality, for each of  $N$  oscillators  $g^2$  can be different according to spatial position and orientation. In SEIRA and SEIRS of molecular layers and nanofilms a complete splitting is not observed, which indicates  $g$  values relevant for weak coupling. A typical mid IR antenna resonance width corresponds to  $\gamma_{pp}/4 \approx 20$  meV  $> g$  for weak coupling.

### III. EXAMPLES AND APPLICATIONS

#### A. Molecular Monolayers and Signal Enhancement

SEIRA and SEIRS enable extremely sensitive proofs of small amounts of molecules [20], [63], [79], [80]. The broadband enhancement obtained in SEIRA additionally gives clear chemical information since the various modes of the adsorbate can be detected [19], [81]. Maximum SEIRA enhancement is of three orders of magnitude [21], [74], which presents an average value. Enhancement in general concerns a signal size measured as the difference in relative intensity between minimum and maximum of the vibrational signal in the SEIRA/SEIRS spectrum regarding the signal size in a reference spectrum. In the calculation of

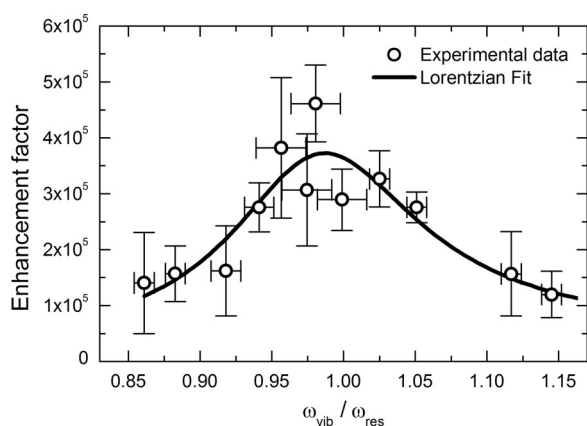


Fig. 10. Enhancement factor (enhanced molecular vibrational signal divided by nonenhanced as derived from IRRAS data, see supporting material to [20]) in dependence on the tuning ratio between vibrational and plasmonic resonance (maximum of resonant extinction). The largest signal enhancement is found close to a ratio of one. Recent studies clarified that maximum enhancement is at the position of the near-field maximum that is slightly shifted from the far-field extinction maximum [75]. Experimental data from electrochemically grown gold nanowires [20], [58].

enhancement factors per molecule, one has to extract first the bare molecular information from the reference spectrum and, second, one has to account for different numbers of molecules that contribute to the signal. In SEIRS usually the localization of near-field enhancement is also considered [82]. In that way for the SEIRS signals in Figs. 8 and 9, maximum enhancement of 500 000 was estimated, see Fig. 10. IR reflection-absorption spectra (IRRAS) from an ODT monolayer on a planar gold surface were used as source for reference data.

With available reference spectra, enhancement per molecule can be estimated from experiments for a known adsorbate coverage and particle geometry. Unfortunately, until now, the enhancement factor cannot be precisely theoretically predicted because of the complex Fano-type effect where disorder not only leads to signal broadening but also signal weakening. One way out was demonstrated recently by a combination of SEIRS that senses a characteristic vibration of the analyte and sensing of the refractive-index the change of which informs on the number of molecules [79]. It should be mentioned here that upon adsorption a plasmonic antenna resonance shifts, but because of the considerable width of the resonance of a nanowire this shift hardly can be measured. In [79], a special asymmetric meta-material structure with extremely narrow plasmonic features was used therefore.

Safe identification of a molecular species with one plasmonic resonance may not be possible if characteristic modes are not within the plasmonic signal. Also, this problem can be solved with the help of complex plasmonic structures that feature a second strong resonance [83] or even more.

Other problems in SEIRS with metal nanoantennas are tiny signals on a huge plasmonic background [50], [84]. S/N can be significantly improved by the use of large homogeneous arrays, but nevertheless the tiny Fano-signals, see Fig. 11, could be overlooked. In the case of available reference data on the bare plasmonic resonance, a baseline correction procedure is

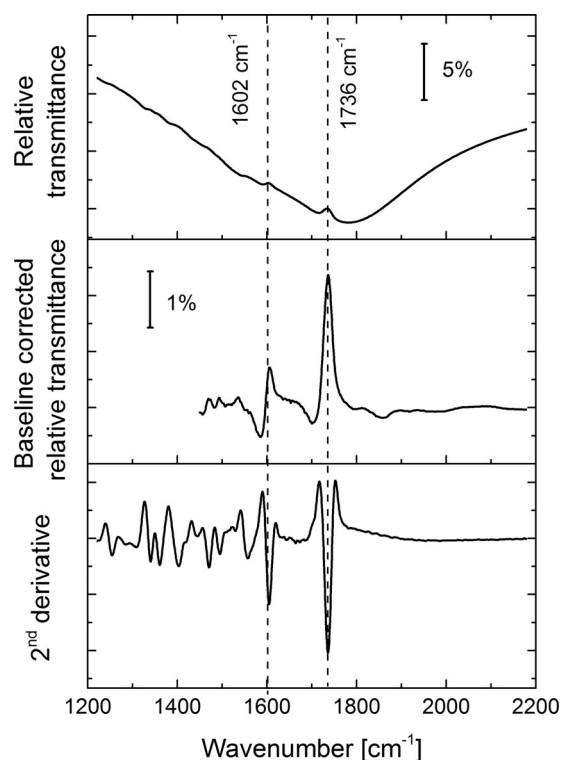


Fig. 11. Relative transmittance spectrum of gold nanoantennas ( $L = 1450$  nm, width and height 60 nm,  $\text{CaF}_2$  substrate) covered with a methylene blue monolayer [84]. In the middle panel, a baseline-correction is obtained using a polynomial fit, whereas in the lower panel the second derivative is calculated. Both the methods are suited to extract hardly visible transmission changes. From the two marked vibrational signals the one at  $1736 \text{ cm}^{-1}$  is not a mode of the free molecules. This mode arises upon adsorption on gold or due to degradation and is a typical example for chemical effects. In our example, the mode appears quite strong because it is close to the plasmonic resonance.

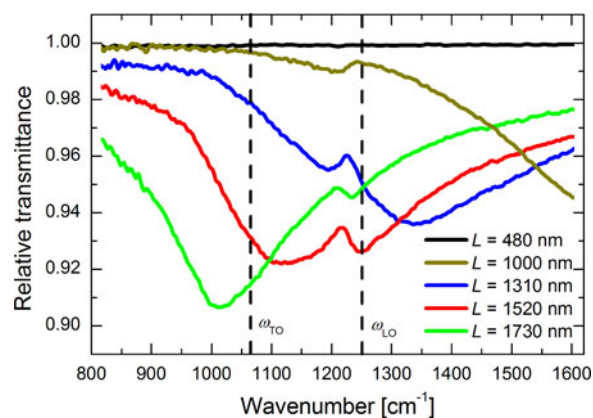


Fig. 12. Relative transmittance spectra of nanoantennas ( $L$  as given) prepared on a Si wafer with a natural  $\text{SiO}_2$  layer (thickness 3 nm). Reference is the oxide-covered wafer without antennas [85].

possible. Otherwise, derivatives can be checked, see for example Fig. 11.

### B. Polariton Sensing of Thin Oxide Films

Nanoantennas prepared on silicon wafers show Fano-type features in certain cases [85], see Fig 12. A closer look on series of spectra for various  $L$  in Fig. 12 identifies the origin of the

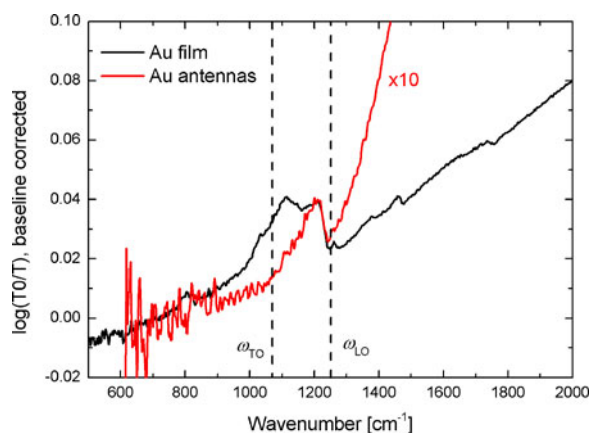


Fig. 13. Comparison of SiO<sub>2</sub> signal enhancement provided by antennas (red) and Au-island films (black). From the relative transmittance, absorption was calculated and, for the black curve, also a baseline correction was done. The red antenna spectrum is multiplied by a factor of 10 to make clear the differences.

feature as phonon–polariton of the natural SiO<sub>2</sub> layer (about 3 nm thick) that couples to the plasmonic excitation. As could be seen from Fig. 1, top panel, SiO<sub>2</sub> has a strong TO phonon oscillator at 1065 cm<sup>-1</sup> that yields a large splitting between TO and LO frequencies and a negative real part of dielectric function in between. In that range surface phonon–polaritons can exist, at the surface and at the interface of a layer to the substrate [12]. The surface polariton branch approaches  $\omega_{LO}$ , and leads to the observed feature. For the interface polariton, interaction with the antenna is less likely [85]. Since the surface polariton has a wave vector parallel to the surface but the incident light has a wave vector perpendicular to the surface, absorption (needs wave-vector conservation) could not explain the phonon–polariton excitation. Clearly, scattering by the nanoantenna gives the wave vector parallel to the surface. Enhanced absorption only can lead to a signal at the TO frequency  $\omega_{TO}$ . Let us again consider gold-island layers on natural oxide (see Figs. 1 and 13). Fig. 13 displays one spectrum from Fig. 1 (for a macroscopic sample area) and one spectrum from Fig. 11 (for the array with shortest antennas, microspectroscopy) in terms of extinction (for a better comparison). The surface polariton excitation is obvious in both the spectra, whereas for the island layer the excitation feature extends down to the TO frequency indicating absorption enhancement of nearly the same amount as scattering enhancement. We conclude that for the antenna (even on the resonance tail) SEIRS from scattering dominates while for the island layer absorption and scattering nearly equally contribute to vibrational signal enhancement. We have to add here, that a scattering contribution from island layers could be detected rather seldom. Usually islands are too small. For metals like iron, with high electronic damping, a scattering contribution was never proven in SEIRA experiments; a Fano-type signal only at  $\omega_{TO}$  was observed [86].

#### IV. CONCLUSION

We have discussed SEIRA with metal-island films and SEIRS with nanoantennas as Fano-type effects in resonant absorption

and scattering, respectively, of plasmonic objects. Our discussion is based on selected literature and own studies. The conclusions are these: maximizing plasmonic enhancement needs strongly scattering plasmonic objects with resonances tuned to the vibrational frequencies of interest. Molecules of interest should sit in an ordered manner on sites with concentrated near-field. Order in principle could be supported by a proper functionalization of smooth antenna surfaces. Until now experiments have demonstrated that the detection limit can be extended down to the zeptomolar range. This is not a general limit. Further improvement of sensitivity and of quantitative analysis mainly needs detailed theoretical work on the role of disorder and coupling and on the interplay of absorption and scattering.

#### ACKNOWLEDGMENT

The authors would like to thank J. Bochterle and S. Wetzel (Heidelberg), H. V. Chung and T. Naggo (Tsukuba), A. Otto (Düsseldorf/Poltersdorf), J. Aizpurua (Donostia-San Sebastian), H. Giessen (Stuttgart), R. Hillenbrand (Donostia-San Sebastian), and P. Nordlander (Rice University) for fruitful discussion.

#### REFERENCES

- [1] D. W. Berreman, "Infrared absorption at longitudinal optic frequency in cubic crystal films," *Phys. Rev.*, vol. 130, no. 6, pp. 2193–2198, Jun. 1963.
- [2] T. Glaser, M. Binder, C. Lennartz, C. Schildknecht, and A. Pucci, "Infrared spectroscopic growth studies of an organic semiconductor," *Phys. Status Solid. A*, vol. 208, no. 8, pp. 1873–1878, Apr. 2011.
- [3] D. Nanova, S. Beck, A. Fuchs, T. Glaser, C. Lennartz, W. Kowalsky, A. Pucci, and M. Kroeger, "Charge transfer in thin films of donor-acceptor complexes studied by infrared spectroscopy," *Org. Electron.*, vol. 13, no. 7, pp. 1237–1244, Apr. 2012.
- [4] B. Bröker, O. T. Hofmann, G. M. Rangger, P. Frank, R.-P. Blum, R. Rieger, L. Venema, A. Vollmer, K. Müllen, J. P. Rabe, A. Winkler, P. Rudolf, E. Zojer, and N. Koch, "Density-dependent reorientation and rehybridization of chemisorbed conjugated molecules for controlling interface electronic structure," *Phys. Rev. Lett.*, vol. 104, no. 24, art no. 246805, pp. 1–4, Jun. 2010.
- [5] T. W. Cornelius, M. E. Toimil-Molares, R. Neumann, G. Fahsold, R. Lovrincic, A. Pucci, and S. Karim, "Quantum size effects manifest in infrared spectra of single bismuth nanowires," *Appl. Phys. Lett.*, vol. 88, no. 10, p. 103114, Mar. 2006.
- [6] H. V. Chung, C. J. Kubber, G. Han, S. Rigamonti, D. Sanchez-Portal, D. Enders, A. Pucci, and T. Nagao, "Optical detection of plasmonic and interband excitations in 1-nm-wide indium atomic wires," *Appl. Phys. Lett.*, vol. 96, no. 24, p. 243101, Jun. 2010.
- [7] Z. Q. Li, E. A. Henriksen, Z. Jiang, Z. Hao, M. C. Martin, P. Kim, H. L. Stormer, and D. N. Basov, "Band structure asymmetry of bilayer graphene revealed by infrared spectroscopy," *Phys. Rev. Lett.*, vol. 102, no. 3, p. 037403, Jan. 2009.
- [8] P. M. Hare, C. T. Middleton, K. I. Mertel, J. M. Herbert, and Bern Kohler, "Time-resolved infrared spectroscopy of the lowest triplet state of thymine and thymidine," *Chem. Phys.*, vol. 347, no. 1–3, pp. 383–392, May 2008.
- [9] N. Ocelic and R. Hillenbrand, "Subwavelength-scale tailoring of surface phonon polaritons by focused ion-beam implantation," *Nat. Mater.*, vol. 3, pp. 606–609, Sep. 2004.
- [10] Z. Zhang, L. Piatkowski, H. J. Bakker, and M. Bonn, "Ultrafast vibrational energy transfer at the water/air interface revealed by two-dimensional surface vibrational spectroscopy," *Nat. Chem.*, vol. 3, pp. 888–893, Nov. 2011.
- [11] C. F. Bohren and D. R. Huffman, *Absorption and Scattering of Light by Small Particles*. Berlin, Germany: Wiley-VCH, 1998.
- [12] A. V. Zayatsa, I. I. Smolyaninov, and A. A. Maradudin, "Nano-optics of surface plasmon polaritons," *Phys. Rep.*, vol. 408, no. 3–4, pp. 131–314, Mar. 2005.

- [13] P. Biagioni, J.-S. Huang, and B. Hecht, "Nanoantennas for visible and infrared radiation," *Rep. Prog. Phys.*, vol. 75, art no. 024402, pp. 1–40, Jan. 2012.
- [14] N. Calandra and M. Willander, "Theory of surface-plasmon resonance optical-field enhancement at prolate spheroids," *J. Appl. Phys.*, vol. 92, no. 9, pp. 4878–4884, Nov. 2002.
- [15] M. Schnell, A. Garcia-Etxarri, J. Alkorta, J. Aizpurua, and R. Hillenbrand, "Phase-resolved mapping of the near-field vector and polarization state in nanoscale antenna gaps," *Nano Lett.*, vol. 10, no. 9, pp. 3524–3528, Nov. 2010.
- [16] M. Pelton, J. Aizpurua, and G. Bryant, "Metal-nanoparticle plasmonics," *Laser Photon. Rev.*, vol. 2, no. 3, pp. 136–159, Apr. 2008.
- [17] D. Weber, P. Albella, P. Alonso-González, F. Neubrech, H. Gui, T. Nagao, R. Hillenbrand, J. Aizpurua, and A. Pucci, "Longitudinal and transverse coupling in infrared gold nanoantenna arrays: Long range versus short range interaction regimes," *Opt. Express*, vol. 19, no. 16, pp. 15047–15061, Aug. 2011.
- [18] O. Krauth, G. Fahsold, and A. Pucci, "Asymmetric line shapes and surface enhanced infrared absorption of CO adsorbed on thin iron films on MgO(001)," *J. Chem. Phys.*, vol. 110, no. 6, pp. 3113–3118, Feb. 1999.
- [19] A. Priebe, M. Sinter, G. Fahsold, and A. Pucci, "The correlation between film thickness and adsorbate line shape in surface enhanced infrared absorption," *J. Chem. Phys.*, vol. 119, no. 9, pp. 4887–4891, Sep. 2003.
- [20] F. Neubrech, A. Pucci, T. W. Cornelius, S. Karim, A. Garcia-Etxarri, and J. Aizpurua, "Resonant plasmonic and vibrational coupling in a tailored nanoantenna for infrared detection," *Phys. Rev. Lett.*, vol. 101, no. 15, p. 157403, Oct. 2008.
- [21] D. Enders, T. Nagao, A. Pucci, T. Nakayama, and M. Aono, "Surface-enhanced ATR-IR spectroscopy with interface-grown plasmonic gold-island films near the percolation threshold," *Phys. Chem. Phys.*, vol. 13, no. 11, pp. 4935–4941, Feb. 2011.
- [22] F. Abeles, "Optical properties of metals," in *Optical Properties of Solids*, F. Abeles, Ed. New York: North-Holland Pub. Co., 1972, pp. 93–162.
- [23] B. E. Sernelius, *Surface Modes in Physics*. Berlin, Germany: Wiley-VCH, 2001.
- [24] V. I. Silin, S. A. Voronov, V. A. Yakovlev, and G. N. Zhizhin, "IR surface plasmon (polariton) phase spectroscopy," *Int. J. Infrared Millimeter Waves*, vol. 10, no. 1, pp. 101–120, Jan. 1989.
- [25] D. V. Fedorov, G. Fahsold, A. Pucci, P. Zahn, and I. Mertig, "Mobility of conduction electrons in ultrathin Fe and Cu films on Si(111)," *Phys. Rev. B*, vol. 75, no. 25, art no. 245427, pp. 1–5, Jun. 2007.
- [26] A. Pucci, F. Kost, G. Fahsold, and M. Jalochowski, "Infrared spectroscopy of Pb layer growth on Si(111)," *Phys. Rev. B*, vol. 74, no. 12, art no. 125428, pp. 1–6, Sep. 2006.
- [27] R. Lovrinčić and A. Pucci, "Infrared optical properties of chromium nanoscale films with a phase transition," *Phys. Rev. B*, vol. 80, no. 20, art no. 205404, pp. 1–6, Nov. 2009.
- [28] K. E. Cilwa, K. R. Rodríguez, J. M. Heer, M. A. Malone, L. D. Corwin, and J. V. Coe, "Propagation lengths of surface plasmon polaritons on metal films with arrays of subwavelength holes by infrared imaging spectroscopy," *J. Chem. Phys.*, vol. 131, no. 6, art no. 061101, pp. 1–5, Aug. 2009.
- [29] N. W. Ashcroft and N. D. Mermin, *Solid State Physics*. Orlando, FL: Saunders College Publishing, 1976.
- [30] A. Otto, "Excitation of nonradiative surface plasma waves in silver by the method of frustrated total reflection," *Z. Physik*, vol. 216, no. 4, pp. 398–410, 1968.
- [31] B. Liedberg, C. Nylander, and I. Lunström, "Surface plasmon resonance for gas detection and biosensing," *Sens. Actuators*, vol. 4, pp. 299–304, 1983.
- [32] J. Homola, "Surface plasmon resonance sensors for detection of chemical and biological species," *Chem. Rev.*, vol. 108, no. 2, pp. 462–493, Jan. 2008.
- [33] S. Maier, *Plasmonics: Fundamentals and Applications*. New York: Springer, 2007.
- [34] J.-C. Weeber, A. Dereux, C. Girard, J. R. Krenn, and J.-P. Goujonnet, "Plasmon polaritons of metallic nanowires for controlling submicron propagation of light," *Phys. Rev. B*, vol. 60, no. 12, pp. 9061–9068, Sep. 1999.
- [35] T. Kalkbrenner, U. Håkanson, and V. Sandoghdar, "Tomographic plasmon spectroscopy of a single gold nanoparticle," *Nano Lett.*, vol. 4, no. 12, pp. 2309–2314, Oct. 2004.
- [36] K.-P. Chen, V. P. Drachev, J. D. Borneman, A. V. Kildishev, and V. M. Shalaev, "Drude relaxation rate in grained gold nanoantennas," *Nano Lett.*, vol. 10, no. 3, pp. 916–922, Mar. 2010.
- [37] L. Novotny, "Effective wavelength scaling for optical antennas," *Phys. Rev. Lett.*, vol. 98, no. 26, p. 266802, Jun. 2007.
- [38] F. Wang and Y. R. Shen, "General properties of local plasmons in metal nanostructures," *Phys. Rev. Lett.*, vol. 97, no. 20, p. 206806, Nov. 2006.
- [39] E. S. Kooij, W. Ahmed, H. J. W. Zandvliet, and B. Poelsema, "Localized plasmons in noble metal nanospheroids," *J. Phys. Chem. C*, vol. 115, no. 21, pp. 10321–10332, May 2011.
- [40] B. Luk'yanchuk, N. I. Zheludev, S. A. Maier, N. J. Halas, R. Nordlander, H. Giessen, and C. T. Chong, "The fano resonance in plasmonic nanostructures and metamaterials," *Nat. Mater.*, vol. 9, pp. 707–715, Sep. 2010.
- [41] N. A. Mirin, K. Bao, and P. Nordlander, "Fano resonances in plasmonic nanoparticle aggregates," *J. Phys. Chem. A*, vol. 113, no. 16, pp. 4028–4034, Feb. 2009.
- [42] N. Liu, T. Weiss, M. Mesch, L. Langguth, U. Eigenthaler, M. Hirscher, C. Sönnichsen, and H. Giessen, "Planar metamaterial analogue of electromagnetically induced transparency for plasmonic sensing," *Nano Lett.*, vol. 10, no. 4, pp. 1103–1107, Sep. 2010.
- [43] F. Meng and A. Pucci, "Growth of silver on MgO(001) and infrared optical properties," *Phys. Stat. Sol. B*, vol. 244, no. 10, pp. 3739–3749, Oct. 2007.
- [44] R. Lovrinčić, S. Noebel, and A. Pucci, "Infrared monitoring of diamond metalization," *Appl. Spectrosc.*, vol. 65, no. 1, pp. 105–107, Jan. 2011.
- [45] G. Fahsold, A. Bartel, O. Krauth, N. Magg, and A. Pucci, "Infrared optical properties of ultrathin Fe films on MgO(001) beyond the percolation threshold," *Phys. Rev. B*, vol. 61, no. 20, pp. 14108–14113, May 2000.
- [46] G. Fahsold, A. Pucci, and K. H. Rieder, "Growth of Fe on MgO(001) studied by He-atom scattering," *Phys. Rev. B*, vol. 61, no. 20, pp. 8475–8483, May 2000.
- [47] S. Berthier and J. Peiro, "Anomalous infra-red absorption of nanocermet in the percolation range," *J. Phys. Condens. Matter*, vol. 10, no. 16, pp. 3679–3694, Apr. 1998.
- [48] U. K. Chettiar, P. Nyga, M. D. Thoreson, A. V. Kildishev, V. P. Drachev, and V. M. Shalaev, "FDTD modeling of realistic semicontinuous metal films," *Appl. Phys. B—Lasers Optics*, vol. 100, pp. 159–168, Mar. 2010.
- [49] H. Brune, "Microscopic view of epitaxial growth: Nucleation and aggregation," *Surf. Sci. Rep.*, vol. 31, no. 3–4, pp. 121–229, May 1998.
- [50] D. Weber, "Nanogaps for nanoantenna-assisted infrared spectroscopy," thesis, Heidelberg University, Heidelberg, Germany, 2011.
- [51] N. J. Halas, S. Lal, W.-S. Chang, S. Link, and P. Nordlander, "Plasmons in strongly coupled metallic nanostructures," *Chem. Rev.*, vol. 111, pp. 3913–3961, May 2011.
- [52] H. Wang, J. Kundu, and N. J. Halas, "Plasmonic nanoshell arrays combine surface-enhanced vibrational spectroscopies on a single substrate," *Angew. Chem. Int. Ed.*, vol. 46, no. 47, pp. 9040–9044, Oct. 2007.
- [53] J. Aizpurua, G. W. Bryant, L. J. Richter, and F. J. García de Abajo, "Optical properties of coupled metallic nanorods for field-enhanced spectroscopy," *Phys. Rev. B*, vol. 71, no. 23, p. 235420, Jun. 2005.
- [54] J. Zuloaga, E. Prodan, and P. Nordlander, "Quantum description of the plasmon resonances of a nanoparticle dimer," *Nano Lett.*, vol. 9, no. 9, pp. 887–891, Jan. 2009.
- [55] R. Esteban, A. G. Borisov, P. Nordlander, and J. Aizpurua, "Bridging quantum and classical plasmonics with a quantum-corrected model," *Nat. Commun.*, vol. 3, art no. 825, pp. 1–9, May 2012.
- [56] N. Berkovitch, P. Ginzburg, and M. Orenstein, "Concave plasmonic particles: Broad-band geometrical tunability in the near-infrared," *Nano Lett.*, vol. 10, no. 4, pp. 1405–1408, Mar. 2010.
- [57] V. Giannini, A. I. Fernández-Domínguez, Y. Sonnefraud, T. Roschuk, R. Fernández-García, and S. A. Maier, "Controlling light localization and light-matter interactions with nanoplasmonics," *Small*, vol. 6, no. 22, pp. 2498–2507, Nov. 2010.
- [58] F. Neubrech, T. Kolb, R. Lovrinčić, G. Fahsold, A. Pucci, J. Aizpurua, T. W. Cornelius, M. E. Toimil-Molares, R. Neumann, and S. Karim, "Resonances of individual metal nanowires in the infrared," *Appl. Phys. Lett.*, vol. 89, no. 25, p. 253104, Dec. 2006.
- [59] F. Neubrech, D. Weber, R. Lovrinčić, A. Pucci, M. Lopes, T. Toury, and M. Lamy de la Chapelle, "Resonances of individual lithographic gold nanowires in the infrared," *Appl. Phys. Lett.*, vol. 93, no. 16, p. 163105, Oct. 2008.
- [60] F. Neubrech, A. Garcia-Etxarri, D. Weber, J. Bochterle, H. Shen, M. Lamy de la Chapelle, G. W. Bryant, J. Aizpurua, and A. Pucci, "Defect-induced activation of symmetry forbidden infrared resonances in individual metallic nanorods," *Appl. Phys. Lett.*, vol. 96, no. 21, p. 213111, May 2010.
- [61] A. Pucci, F. Neubrech, J. Aizpurua, T. Cornelius, and M. L. Chapelle, "Electromagnetic nanowire resonances for field-enhanced spectroscopy," in *One-Dimensional Nanostructures*, Z. M. Wang, Ed. New York: Springer, 2008, pp. 175–215.



- [62] M. Schnell, A. García-Etxarri, A. J. Huber, K. Crozier, J. Aizpurua, and R. Hillenbrand, "Controlling the near-field oscillations of loaded plasmonic nanoantennas," *Nature Photonics*, vol. 3, pp. 287–291, Apr. 2009.
- [63] R. Adato, A. A. Yanik, J. J. Amsden, D. L. Kaplan, F. G. Omenetto, M. K. Hong, S. Erramilli, and H. Altug, "Ultra-sensitive vibrational spectroscopy of protein monolayers with plasmonic nanoantenna arrays," in *Proc. Natl. Acad. Sci.*, Nov. 2009, vol. 106, no. 46, pp. 19227–19232.
- [64] R. Bukasov and J. S. Shumaker-Parry, "Silver nanocrescents with infrared plasmonic properties as tunable substrates for surface enhanced infrared absorption spectroscopy," *Anal. Chem.*, vol. 81, no. 11, pp. 4531–4535, Jun. 2009.
- [65] A. Pucci, "IR spectroscopy of adsorbates on ultrathin metal films," *Phys. Stat. Sol. B*, vol. 242, no. 13, pp. 2704–2713, Oct. 2005.
- [66] V. Liberman, R. Adato, A. Mertiri, A. A. Yanik, K. Chen, T. H. Jeys, S. Erramilli, and H. Altug, "Angle-and polarization-dependent collective excitation of plasmonic nanoarrays for surface enhanced infrared spectroscopy," *Opt. Express*, vol. 19, no. 12, pp. 11202–11212, Jun. 2011.
- [67] A. E. Miroschnichenko, S. Flach, and Y. S. Kivshar, "Fano resonances in nanoscale structures," *Rev. Modern Phys.*, vol. 82, no. 3, pp. 2257–2298, Jul.–Sep. 2010.
- [68] V. Giannini, Y. Francescato, H. Amrania, C. C. Phillips, and S. A. Maier, "Fano resonances in nanoscale plasmonic systems: A parameter-free modeling approach," *Nano Lett.*, vol. 11, no. 7, pp. 2835–2840, Jun. 2011.
- [69] M. Kroner, A. O. Govorov, S. Remi, B. Biedermann, S. Seidl, A. Badolato, P. M. Petroff, W. Zhang, R. Barbour, B. D. Gerardot, R. J. Warburton, and K. Karrai, "The nonlinear fano effect," *Nature*, vol. 451, pp. 311–314, Jan. 2008.
- [70] A. Priebe, G. Fahsold, and A. Pucci, "Strong pyramidal growth of metal films studied with IR transmittance and surface enhanced IR absorption of CO," *J. Phys. Chem. B*, vol. 108, no. 47, pp. 18174–18178, Nov. 2004.
- [71] M. Sinther, A. Priebe, and A. Pucci, to be published.
- [72] E. Cubukcu I, S. Zhang, Y.-S. Park, G. Bartal, and X. Zhang, "Split ring resonator sensors for infrared detection of single molecular monolayers," *Appl. Phys. Lett.*, vol. 95, no. 4, p. 043113, Jul. 2009.
- [73] P. Alonso-González, P. Albella, M. Schnell, J. Chen, F. Huth, A. García-Etxarri, F. Casanova, F. Golmar, L. Arzubiza, L. E. Hueso, J. Aizpurua, and R. Hillenbrand, "Resolving the electromagnetic mechanism of surface-enhanced light scattering at single hot spots," *Nat. Commun.*, vol. 3, pp. 1–7, Feb. 2012.
- [74] D. Enders and A. Pucci, "Surface enhanced infrared absorption of octadecanethiol on wet-chemically prepared Au nanoparticle films," *Appl. Phys. Lett.*, vol. 88, no. 18, p. 184104, May 2006.
- [75] P. Alonso-González, P. Albella, F. Neubrech, J. Chen, F. Golmar, F. Casanova, L. E. Hueso, A. Pucci, J. Aizpurua, and R. Hillenbrand, "Experimental verification of the spectral shift between near- and far-field peak intensities of plasmonic infrared nanoantennas," to be published.
- [76] A. Manjavacas, F. J. García de Abajo, and P. Nordlander, "Quantum plexcitons: Strongly interacting plasmons and excitons," *Nano Lett.*, vol. 11, no. 6, pp. 2318–2323, May 2011.
- [77] S. Savasta, R. Saija, A. Ridolfo, O. Di Stefano, P. Denti, and F. Borghese, "Nanopolaritons: Vacuum Rabi splitting with a single quantum dot in the center of a dimer nanoantenna," *ACS Nano*, vol. 4, no. 11, pp. 6369–6376, Oct. 2010.
- [78] W. Petrich, "Mid-infrared and Raman spectroscopy for medical diagnostics," *Appl. Spect. Rev.*, vol. 36, no. 2–3, pp. 181–237, Oct. 2001.
- [79] C. Wu, A. B. Khanikaev, R. Adato, N. Arju, A. A. Yanik, H. Altug, and G. Shvets, "Fano-resonant asymmetric metamaterials for ultrasensitive spectroscopy and identification of molecular monolayers," *Nat. Mater.*, vol. 11, pp. 69–75, Jan. 2012.
- [80] S. Cataldo, J. Zhao, F. Neubrech, B. Frank, C. Zhang, P. V. Braun, and H. Giessen, "Hole-mask colloidal nanolithography for large-area low-cost metamaterials and antenna-assisted surface-enhanced infrared absorption substrates," *ACS Nano*, vol. 6, no. 1, pp. 979–985, Jan. 2012.
- [81] M. Sinther, A. Pucci, A. Otto, A. Priebe, S. Diez, and G. Fahsold, "Enhanced infrared absorption of SERS-active lines of ethylene on Cu," *Phys. Stat. Sol. A*, vol. 188, no. 4, pp. 1471–1476, Dec. 2001.
- [82] EPAPS Document No. E-PRLTAO-101-036842, supplementary material to [20].
- [83] K. Chen, R. Adato, and H. Altug, "Dual band perfect absorber for multi-spectral plasmon-enhanced infrared spectroscopy," *ACS Nano*, vol. 6, no. 9, pp. 7998–8006, Aug. 2012.
- [84] C. D'Andrea, J. Bochterle, A. Toma, F. Neubrech, E. Di Fabrizio, P. G. Gucciardi, and A. Pucci, "Optical nanoantennas as common substrates for SERS and SEIRS," to be published.
- [85] F. Neubrech, D. Weber, D. Enders, T. Nagao, and A. Pucci, "Antenna sensing of surface phonon polaritons," *J. Phys. Chem. C*, vol. 114, no. 16, pp. 7299–7301, Feb. 2010.
- [86] S. Wetzel, "Infrarotspektroskopische Untersuchung von Siliziumoxiden, Silikaten, deren Wechselwirkung mit Metallpartikeln sowie Dampfdruckmessungen an Siliziummonoxid," thesis, Heidelberg University, Heidelberg, Germany, 2012.



**Frank Neubrech** was born in Kaiserslautern, Germany, in 1981. He received the Diploma degree in physics from the University of Kaiserslautern, Kaiserslautern, Germany, and the University of Heidelberg, Heidelberg, Germany, in 2006 and the Doctorate degree (*summa cum laude*) in Prof. A. Pucci's group at the Kirchhoff-Institute for Physics, University Heidelberg, in 2008, where he investigated a new approach to surface enhanced infrared absorption using metal nanoparticles that allows an ultrasensitive spectral detection of molecular vibrations down to

atto-molar concentrations.

Since 2008, he has been a Postdoctoral Researcher in Prof. Pucci's group on the application of surface enhanced infrared spectroscopy to early disease diagnosis. Besides this research, he is also involved in other projects dealing with experimental and theoretical aspects of plasmonics and field enhanced spectroscopic methods. Since October 2012, he has also been a Postdoctoral Researcher in Prof. H. Giessen's group at the Stuttgart University, Stuttgart, Germany.



**Annemarie Pucci** was born in Weimar, Thuringia, Germany, in 1954. She received the Diploma degree in physics from Friedrich-Schiller University Jena, Thuringia, Germany, in 1977, the Doctorate degree (*summa cum laude*) from the Department of Physics, University of Rostock, Mecklenburg, Germany, in 1983, where her research was focused on the field of the theory of phonons in disordered materials, and the Habilitation degree from Friedrich-Schiller University Jena, in 1992, where her habilitation thesis was focused on experimental IR spectroscopy at the same time and applying it to gate oxide layer studies and later to optical layers.

In 1991, she was with the Department of Physics, Free University of Berlin, Berlin, Germany, where she performed surface-phonon studies with He-atom beams under UHV conditions, together with K.-H. Rieder. Since 1995, she has been a Full Professor of experimental physics at Heidelberg University, Heidelberg, Germany. Her research interests include studies of excitations of various nanostructures and thin layers in the IR energy range. Her main focus is on studies of interactions at interfaces with surface-enhanced IR spectroscopy as one example.